Reduction of Mercury(II) by the Carbon Dioxide Radical Anion: A Theoretical and Experimental Investigation

Andrea M. Berkovic,[†,‡] Mónica C. Gonzalez,[†] Nino Russo,[§] María del Carmen Michelini,[§] Reinaldo Pis Diez,[*,‡] and Daniel O. Mártire[*,†]

Instituto de Investigaciones Fisicoquímicas Teóricas y Aplicadas (INIFTA), Facultad de Ciencias Exactas, Universidad Nacional de La Plata, Casilla de Correo 16, Sucursal 4, 1900 La Plata, Argentina, Centro de Química Inorgánica (CEQUINOR, CONICET/UNLP), Facultad de Ciencias Exactas, Universidad Nacional de la Plata, Casilla de Correo 962, B1900AVV La Plata, Argentina, and Dipartimento di Chimica, Università della Calabria, Via P. Bucci, Cubo 14 C, 87030 Arcavacata di Rende, Italy

Received: June 30, 2010; Revised Manuscript Received: October 26, 2010

The laser flash photolysis technique ($\lambda_{exc} = 266$ nm) was used to investigate the mechanism of the $HgCl_2$ reduction mediated by $CO_2^{\bullet-}$ radicals in the temperature range 291.7−308.0 K. For this purpose, the $CO_2^{\bullet-}$ radicals were generated by scavenging of sulfate radicals by formic acid. The absorbance of the reduced radical of methyl viologen, a competitive scavenger of $CO_2^{\bullet-}$, was monitored at 390 nm. Moreover, theoretical calculations, including solvent effects, were also performed within the framework of the density functional theory for various chemical species of Hg(I) and Hg(II) to aid in the modeling of the reaction of reduction of $HgCl_2$ by $CO_2^{\bullet-}$.

Introduction

The toxicity of mercury is one of the most severe known. It is released to the atmosphere mainly from fossil fuel combustion but also from natural sources such as volcanic activities. In the atmosphere, mercury is transported and transformed into several species with different properties.[1]

The chemical reduction of Hg(II) in the aqueous phase may influence the pool of elemental mercury in aqueous atmospheric and terrestrial compartments and the physical processes regulating its flux to the gaseous phase.[2]

Various biological, chemical, and physical methods have been used for contaminated site remediation. One such cleanup method is in situ chemical oxidation (ISCO), in which strong oxidants are injected into the subsurface. The oxidants react with the contaminants, producing substances such as carbon dioxide, water, and, in the case of compounds containing heteroatoms, inorganic acids. The newest and least explored ISCO reagent is peroxodisulfate. Peroxodisulfate oxidation is generally carried out under heat-activated, photoactivated, acid-activated, base-activated, or metal-activated conditions to form $SO_4^{\bullet-}$ radicals.[3−5]

Photolysis of $S_2O_8^{2-}$ is a clean source for $SO_4^{\bullet-}$ radical anions with high pH-independent quantum yields:[6,7]

$$S_2O_8^{2-} + h\nu \rightarrow 2SO_4^{\bullet-} \quad (1)$$

Sodium formate was proposed as an additive to transform the oxidative peroxodisulfate medium into a reductive one. The effect of this additive is due to the reaction of the sulfate radicals ($SO_4^{\bullet-}$) with formate ions and formic acid to yield the reductive $CO_2^{\bullet-}$ radicals ($\lambda^{max} = 235$ nm, $\varepsilon(235\text{nm}) = 3000$ M^{-1} cm^{-1}):[8−11]

$$SO_4^{\bullet-} + (HCO_2^-/HCOOH) \rightarrow SO_4^{2-} + CO_2^{\bullet-} + (H^+ + 2H^+) \quad (2)$$

The $CO_2^{\bullet-}$radicals have a reduction potential of $E(CO_2/CO_2^{\bullet-}) \approx -2$ V versus NHE[12] and should be therefore able to initiate a one-electron reduction of $HgCl_2$ in solution ($E(HgCl_2/HgCl) = -0.47$ V at $[Cl^-] = 0.05$ M).[13]

Thus, we employed here the laser flash photolysis technique ($\lambda_{exc} = 266$ nm) with Ar-saturated peroxodisulfate solutions of pH = 1−2 in the presence of formic acid to investigate the mechanism of the $HgCl_2$ reduction mediated by $CO_2^{\bullet-}$ radicals. Moreover, theoretical calculations, including solvent effects, were also performed within the framework of the density functional theory for various chemical species of Hg(I) and Hg(II) to aid in the modeling of the reaction of reduction of $HgCl_2$ by $CO_2^{\bullet-}$.

Materials and Methods

Materials. $Na_2S_2O_8$, NaHCOO, HCOOH, $HClO_4$, $CHCl_3$, $HgCl_2$, Na_2HPO_4, KBr, K_2CO_3, and H_2SO_4 (all from J. T. Baker), $KMnO_4$ (Anedra), Na_2SO_4 (Anedra), methyl viologen dichloride ($(MV)Cl_2$; from Aldrich), and hydroxylamine hydrochloride and dithizone (both from Fluka) were used without further purification. Deionized water (>18 MΩ cm, <20 ppb organic carbon) was obtained from a Millipore system.

Because diluted mercury solutions undergo losses during storage, all mercury working solutions were freshly prepared prior to each experiment.

The temperature of the solutions was controlled to ±1 K with a Grant model GD 1200 thermostat.

* To whom correspondence should be addressed. Tel.: (+54) 221 424 0172 (R.P.D.); (+54) 221 4257430/7291 (D.O.M.). Fax: (+54) 221 424 0172 (R.P.D.); (+54) 221 4254642 (D.O.M.). E-mail: pis_diez@quimica.unlp.edu.ar (R.P.D.); dmartire@inifta.unlp.edu.ar (D.O.M.).

† INIFTA, Universidad Nacional de la Plata.

‡ CEQUINOR, CONICET/UNLP, Universidad Nacional de la Plata.

§ Università della Calabria (Fax: (+39) 0984 493 390).

10.1021/jp106035m
Published on Web 11/18/2010

Laser Flash Photolysis Experiments. Laser flash photolysis (LFP) experiments were performed by excitation with the fourth harmonic of a Nd:YAG Litron laser (2 ns full width at half-maximum (fwhm) and 6 mJ/pulse at 266 nm). The analysis light from a 150 W Xe arc lamp was passed through a monochromator (PTI 1695) and detected by a 1P28 PMT photomultiplier. A 10 mm path length cuvette was employed.[14] Decays typically represented the average of 64 pulses and were taken by and stored in a 500 MHz Agilent Infiniium oscilloscope. The solutions had an absorbance of 0.5 at 266 nm, and less than 1% of the incident light was absorbed by $HgCl_2$, HCOOH, and methyl viologen, which guarantees that photolysis of these substances is negligible under our experimental conditions.

Due to the high absorbance of the solutions below 300 nm, the direct detection of $CO_2^{\bullet -}$ and of Hg(I)[15] was not possible. Thus, since the $CO_2^{\bullet -}$ radicals are able to reduce methyl viologen (MV^{2+}) to the $MV^{\bullet +}$ radical ($\lambda^{max} = 393$ nm[16]), MV^{2+} was employed as a probe.

Continuous Irradiation Experiments. Ar-saturated aqueous solutions containing 5×10^{-2} M $Na_2S_2O_8$, 0.4 M NaCOOH or HCOOH, and 1×10^{-4} M Hg(II) (pH = 1 or 2) were irradiated either with the laser at 266 nm in a 1 cm path length quartz fluorescence cuvette or with a 125 W HPK mercury lamp in a 750 mL glass reactor equipped with a quartz jacket. Solutions contained in the reactor were continuously bubbled with Ar during the experiment.

Solutions irradiated with the laser were prepared with deionized water. To check the possibility of applying the Hg(II) reduction/precipitation method to drinking water, solutions to be irradiated with the lamp were also prepared with drinking water obtained from groundwater. The physicochemical analysis of the drinking water employed for these experiments is shown in Supporting Information Table S1.

The lamp ferrioxalate actinometry[17] yielded 1.57×10^{20} quanta/s at the controlled temperature of 23 °C. The photolysis times were shorter than 3 h. The irradiated solutions were centrifuged at 5000 rpm for 45 min. Hg(II) was quantified in the supernatant by a colorimetric method with dithizone (EPA 3500-Hg C, detection wavelength of the complex = 492 nm). Total mercury analysis was performed by cold vapor atomic absorption (EPA SW 846 M 7470 EAA cold vapor) with Varian Spectraa-55 equipment.

Theoretical Methodology. To get an insight into the role of the $CO_2^{\bullet -}$radical in the one-electron reduction of $HgCl_2$ in solution, various complexes formed by Hg(II) and Hg(I) with H_2O and Cl^- were investigated. In particular, the species $Hg(H_2O)_m^{2+}$ ($m = 1-6$), $HgCl_m^{2-m}$ ($m = 1-5$), $Hg_2(H_2O)_m^{2+}$ ($m = 2, 4$), and $Hg_2Cl_m^{2-m}$ ($m = 2, 4$) were studied in detail using the three-parameter hybrid exchange-correlation B3LYP functional[18,19] within the framework of the density functional theory (DFT).[20−22] The basis sets cc-pVTZ-PP[23,24] and cc-pVTZ[25] were used for mercury and the rest of the atoms, respectively. The Hg(I) complex HgCl was also studied to test some suggestions made in the literature.[13] Various starting geometries were considered for the Hg(II) complexes. Optimizations were carried out without geometric constraints, irrespective of the starting symmetry of each complex. The optimized geometries of the CO_2, $CO_2^{\bullet -}$, and H_2O molecules and the total electronic energy of the Cl^- anion were also obtained at the same level of theory. To validate the above methodology, some optimized bond distances are compared with experimental and calculated data from other sources. The comparison is shown in Supporting Information Table S2.

The eigenvalues of the Hessian matrix were used to determine the zero-point correction to the electronic energies and the corresponding thermal corrections to obtain an estimate of Gibbs energies according to

$$G = E_0 + \Delta E_{0\rightarrow 298} + PV - TS \quad \text{(I)}$$

where $\Delta E_{0\rightarrow 298}$ is the thermal correction to the electronic energy, including the zero-point energy, to go from 0 to 298 K. Those G functions can then be used to obtain standard Gibbs energies of reaction.

Solvent effects (water) were taken into account within the framework of the integral equation formalism for the polarizable continuum model.[26] All the calculations were carried out with the GAUSSIAN03 package.[27]

Results and Discussion

Reaction of the Carbon Dioxide Radical Anion with Mercury(II) Ions. Reaction of $CO_2^{\bullet -}$ ($\lambda^{max} = 235$ nm, $\varepsilon(235\text{nm}) = 3000\ M^{-1}\ cm^{-1}$)[8] with $S_2O_8^{2-}$has been investigated.[28]

The rate constants for the reaction of $CO_2^{\bullet -}$ with Hg(II) were obtained by a modification of the competition method reported in the literature.[29] Since MV^{2+} is known to react with $CO_2^{\bullet -}$ with a rate close to the diffusion limit ($k_4 = (6.3 \pm 0.7) \times 10^9\ M^{-1}\ s^{-1}$),[30,31] and reduced $MV^{\bullet +}$ shows high absorption in the UV and visible,[16] we employed MV^{2+} as a competitive scavenger of $CO_2^{\bullet -}$:

$$CO_2^{\bullet -} + Hg(II) \rightarrow Hg^{\bullet +} + CO_2 \quad (3)$$

$$CO_2^{\bullet -} + MV^{2+} \rightarrow MV^{\bullet +} + CO_2 \quad (4)$$

Under the experimental conditions employed in the LFP experiments (total $[Cl^-] \approx 3 \times 10^{-4}$ M), the aqueous soluble $HgCl_2$ complex is the main Hg(II) species in solution (stability constant = $10^{13.2}$).[32] Formation of mercury(II)−formate complexes is negligible, since, even for low-weight dicarboxylic acids, the Hg(II) complexes with chloride ions present much higher stability constants than those of carboxylic acids.[33] The one-electron reduction of $HgCl_2$ is expected to yield HgCl and chloride anions, was reported for $HgCl_2$ reduction by the solvated electron.[34] Further dimerization of HgCl (reaction 5, $2k_5 = (8.0 \pm 0.5) \times 10^9\ M^{-1}\ s^{-1}$)[34] yields Hg_2Cl_2. The extremely low solubility of the latter product ($K_{sp} = 5 \times 10^{-20}$)[35] ensures its removal from solution, and therefore, it is not involved in further redox reactions.

$$2HgCl \rightarrow Hg_2Cl_2 \quad (5)$$

The $MV^{\bullet +}$ formed in experiments with Ar-saturated 5×10^{-2} M $Na_2S_2O_8$ solutions of pH = 2 containing 1×10^{-4} M MV^{2+} and different concentrations of Hg(II) as monitored at 390 nm. In the absence of Hg(II), $MV^{\bullet +}$ decay follows a second-order rate law, due to radical recombination, reaction 6; see Figure 1.

$$MV^{\bullet +} + MV^{\bullet +} \rightarrow (MV)_2^{2+} \quad (6)$$

Typical $MV^{\bullet +}$ traces in the presence of different amounts of $HgCl_2$ are shown in Figure 2 (inset).

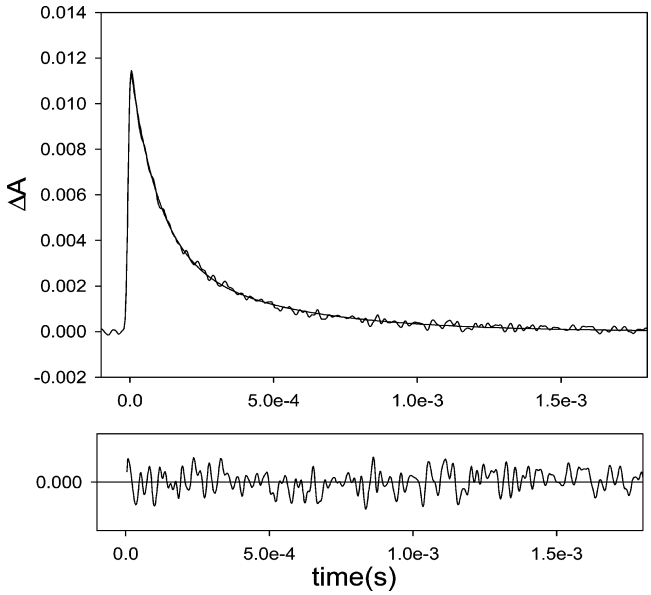

Figure 1. Typical $MV^{\bullet+}$ decay trace ($T = 291.7$ K) obtained at 390 nm with Ar-saturated 5×10^{-2} M $Na_2S_2O_8$ solutions of pH = 2 containing 0.4 M HCOOH, 1×10^{-4} M MV^{2+} in the absence of $HgCl_2$ (where, for example, 5.0e-4 represents 5×10^{-4}). The continuous line shows fitting to the second-order decay function. The corresponding residuals are shown below.

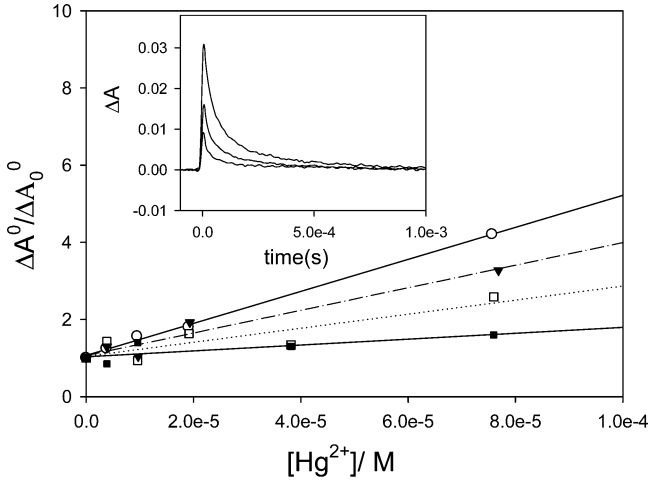

Figure 2. Plots of $\Delta A_0{}^0/\Delta A_0$ vs [Hg(II)] obtained at different temperatures: 291.7 (○), 300.5 (▼), 303.0 (□), and 308.0 K (■) (where, for example, 5.0e-4 represents 5×10^{-4}). Inset: $MV^{\bullet+}$ decay traces ($T = 300.5$ K) obtained at 390 nm with Ar-saturated 5×10^{-2} M $Na_2S_2O_8$ solutions of pH = 2 containing 0.4 M HCOOH, 1×10^{-4} M MV^{2+}, and different concentrations of $HgCl_2$ [Hg(II): 0 (upper trace), 1.9×10^{-4} (middle trace), and 7.7×10^{-5} M (lower trace)].

The absorbance change at $t = 0$, ΔA_0, decreases with increasing initial concentration of Hg(II), $[Hg^{2+}]$, as shown by the linear plots of $\Delta A_0{}^0/\Delta A_0$ vs $[Hg^{2+}]$ obtained in the temperature range 291.7−308.0 K (Figure 1). The amount $\Delta A_0{}^0$ is the value of ΔA_0 measured for $[Hg^{2+}] = 0$.

The decrease of ΔA_0 vs $[Hg^{2+}]$ is given by[29]

$$\frac{\Delta A_0^0}{\Delta A_0} = 1 + \frac{k_3[Hg^{2+}]}{k_4[MV^{2+}]} \qquad \text{(II)}$$

According to eq II the slopes of the linear plots of $\Delta A_0{}^0/\Delta A_0$ vs $[Hg^{2+}]$ equal $k_3/(k_4[MV^{2+}])$. The values of k_3/k_4 obtained from these plots are listed in Table 1.

TABLE 1: Values of k_3/k_4 and k_7 Obtained at Different Temperatures

T (K)	$k_3/k_4{}^a$	$k_7{}^a$ (M^{-1} s^{-1})
291.7	4.2 ± 0.1	$(4 \pm 2) \times 10^7$
300.5	2.9 ± 0.4	$(6 \pm 2) \times 10^7$
303.0	1.8 ± 0.5	$(16 \pm 3) \times 10^7$
308.0	0.8 ± 0.3	$(21 \pm 2) \times 10^7$

[a] The error bars represent the error in the slopes of the corresponding linear plots.

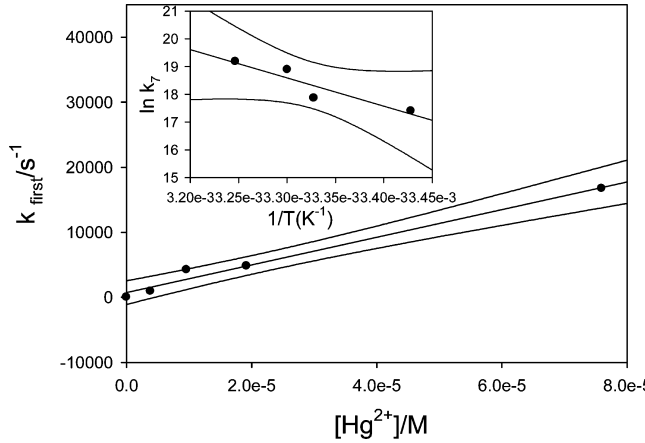

Figure 3. Plot of k_{first} vs [Hg(II)] obtained at 308.0 K (where, for example, 2.0e-5 represents 2.0×10^{-5}). Inset: Arrhenius plot of ln k_7 vs $1/T$. The 95% confidence intervals are shown.

From the slope of the linear plot of $\ln\{k_3/(k_4[MV^{2+}]\}$ vs $(1/T)$ the value of $(E_4 - E_3)/R = (9 \pm 3) \times 10^3$ K, which means that E_4 is 75 ± 25 kJ mol^{-1} greater than E_3.

In the presence of Hg(II), faster $MV^{\bullet+}$ decay rates are observed, and the obtained traces were fitted with a mixed first- and second-order rate law:

$$\Delta A(t) = \frac{k_{first}}{b \exp(k_{first} t) - c} \qquad \text{(III)}$$

$\Delta A(t)$ is the time-dependent absorbance, $c = 2k_6/\varepsilon l$ with ε being the absorption coefficient and $l = 1$ cm, the optical path length; $b = c + k_{first}/\Delta A_0$ with k_{first} being the pseudo-first-order decay rate constant, which strongly depends on $[Hg^{2+}]$. For fitting the data obtained in the presence of Hg(II), the second-order parameter, c, for each experiment was set equal to the value obtained from the experiment performed in the absence of Hg(II) at the same temperature.

Within the experimental error, $k_6 = (1.5 \pm 0.2) \times 10^{10}$ M^{-1} s^{-1} does not depend on the temperature in the range from 291.7 to 308.0 K. The constancy of k_6 in this temperature range indicates a low activation energy for reaction 6. An estimation of the dimerization rate constant $k_6 = 10^4$ M^{-1} s^{-1} at room temperature was obtained from electrochemical measurements.[36] However, should this be the value of k_6 at room temperature, we would not be able to detect a second-order component of the decay of $MV^{\bullet+}$.

The observed linear dependence of k_{first} on $[Hg^{2+}]$ (Figure 3) supports a reaction between $MV^{\bullet+}$ and Hg(II). Reduction of $HgCl_2$, the main mercury species present under our experimental conditions, by $MV^{\bullet+}$ is thermodynamically feasible and is well-documented in the literature.[13] Therefore, from the linear plots of k_{first} vs $[Hg^{2+}]$ the values of the rate constant k_7 at every temperature can be obtained (Table 1).

$$MV^{\bullet+} + HgCl_2 \rightarrow MV^{2+} + HgCl + Cl^- \quad (7)$$

Since in the absence of mercury the reduced radical $MV^{\bullet+}$ decays by second-order kinetics, the intercept of the plot shown in Figure 3 is, within the experimental error, equal to zero.

Reduction of $HgCl_2$ by $MV^{\bullet+}$ was proposed to be reversible; i.e., $MV^{\bullet+} + HgCl_2 \leftrightarrows MV^{2+} + HgCl + Cl^-$ with an equilibrium constant $K_7 = 2.5$ at $[Cl^-] = 0.05$ M.[13] The rate of the reverse reaction (−7) seems to be very low under our experimental conditions probably due to the fast removal of HgCl as Hg_2Cl_2.

$$MV^{2+} + HgCl + Cl^- \rightarrow MV^{\bullet+} + HgCl_2 \quad (-7)$$

The linear plot of ln k_7 vs T^{-1} (see the inset of Figure 3) yields an activation energy $E_7 = 85 \pm 23$ kJmol^{-1}.

Determination of Mercury. The concentration of Hg(II) in Ar-saturated solutions containing 5×10^{-2} M $Na_2S_2O_8$, 0.4 M NaCOOH, and 1×10^{-4} M Hg(II) (pH = 1 or 2) was found to decrease with increasing irradiation times ($\lambda^{exc} = 266$ nm), as shown in Figure 4 (inset). After 1 h irradiation of the solutions, the concentration of Hg(II) decreases to about 1.3×10^{-5} M (2.6 ppm). The results are, within the experimental error, independent of whether the pH was 1 or 2. Moreover, solutions prepared either with deionized or drinking water yield similar results.

The remnant concentration of mercury in solution, $[Hg]_{TOTAL}$, measured by atomic absorption after precipitation of Hg_2Cl_2 (see Materials and Methods), diminishes with the irradiation time, as shown in Figure 4. A 99.8% decrease (from 1.0×10^{-4} to 2.5×10^{-7} M) is observed after 1 h irradiation.

Theoretical Calculations. Figures 5 and 6 show the optimized geometries for the species $Hg(H_2O)_n^{2+}$ ($m = 1-6$), $HgCl_n^{2-n}$ ($m = 2-5$), $Hg_2(H_2O)_2^{2+}$, and $Hg_2Cl_m^{2-m}$ ($m = 2, 4$). The optimized linear geometries of $HgCl^+$ and HgCl are not shown. It should be noted that, even when several starting structures were considered, the geometry of complex $Hg_2(H_2O)_4^{2+}$ could not be optimized. It was observed that, in all cases, two water molecules, one on each Hg(I) ion, tend to move away from the metallic ions. Thus, the species $Hg_2(H_2O)_2^{2+}$ is obtained after the optimization cycle.

For all complexes whose geometries were successfully optimized, binding energies were calculated using total electronic energies, corrected by the zero-point energy in the case of molecules. These results, not shown in the present work, indicate that Hg_2Cl_2, $HgCl_2$, and $Hg(H_2O)_2^{2+}$ are the most stable species in every group, $Hg_2(H_2O)_2^{2+}$ being the only aqueous Hg(I) complex studied. However, because binding energy values are very close to each other, various standard Gibbs energies of reaction were calculated to reinforce the above results with thermodynamic arguments. Table 2 lists standard Gibbs energies for some selected reactions.

It can be seen from the first rows in the table that both $HgCl_2$ and $Hg(H_2O)_2^{2+}$ are the most stable complexes in every group according to the reactions in which water molecules or chloride ions are exchanged. Moreover, $HgCl_2$ is about 92 kJ mol^{-1} more stable than $Hg(H_2O)_2^{2+}$ with respect to the exchange of two water molecules and two chloride ions. The last rows in Table 2 clearly show that Hg_2Cl_2 is more stable than $Hg_2Cl_4^{2-}$ and $Hg_2(H_2O)_2^{2+}$ by about 80 and 57 kJ mol^{-1}, respectively, according to the corresponding reactions. Moreover, HgCl exhibits a strong tendency to dimerize to Hg_2Cl_2; see the last row in Table 2. Thus, the above results clearly suggest that the

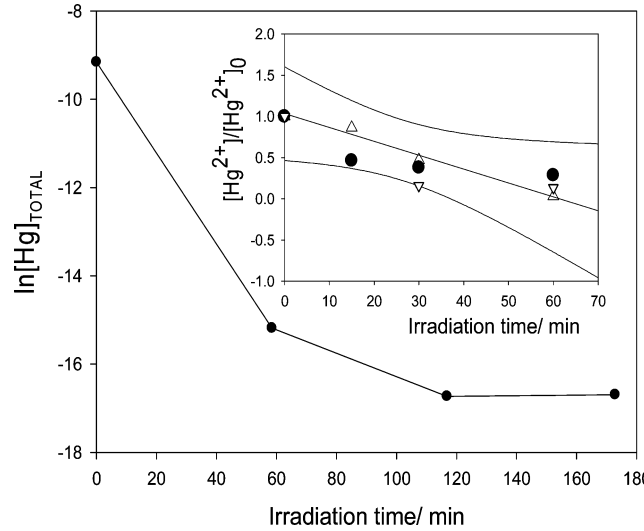

Figure 4. Depletion of $[Hg]_{TOTAL}$ upon irradiation with an HPK mercury lamp of a pH = 2 aqueous solution containing 5×10^{-2} M $Na_2S_2O_8$, 0.4 M HCOOH, and 1×10^{-4} M Hg(II). Inset: Relative depletion of the concentration of Hg(II) upon irradiation ($\lambda^{exc} = 266$ nm) of a 5×10^{-2} M $Na_2S_2O_8$, 0.4 M HCOOH, containing 1×10^{-4} M Hg(II) of pH = 2 (Δ), pH = 1 (●), and pH = 2 (▽, solution prepared with drinking water). The 99% confidence interval is shown.

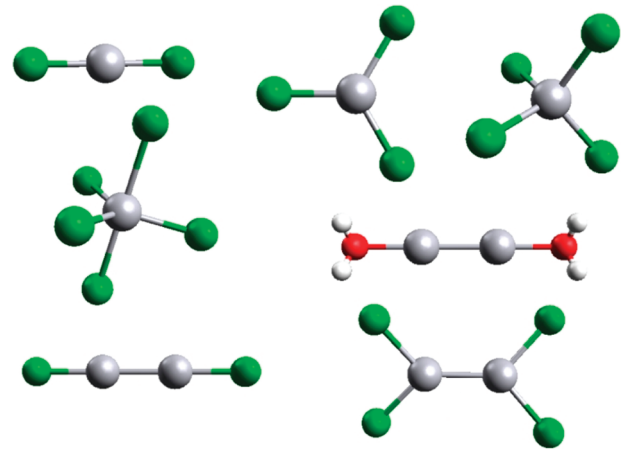

Figure 5. Optimized geometries of $HgCl_m^{2-m}$ ($m = 2-5$), $Hg_2(H_2O)_2^{2+}$, and $Hg_2Cl_m^{2-m}$ ($m = 2, 4$). Gray, green, red, and white spheres represent mercury, chlorine, oxygen, and hydrogen, respectively.

reduction of Hg(II) to Hg(I) by the carbon dioxide radical anion should proceed by a two-electron process according to

$$2CO_2^{\bullet-}(aq) + 2HgCl_2(aq) \rightarrow 2CO_2(aq) + Hg_2Cl_2(aq) + 2Cl^-(aq) \quad (8)$$

The standard Gibbs energy for the above reaction is −464.44 kJ mol^{-1}, which amounts to an electromotive force (EMF) of about 2.41 V. Interestingly, this result compares very well to data obtained from literature for other two-electron processes.[37]

$$2CO_2^{\bullet-}(aq) + 2HgCl_2(s) \rightarrow 2CO_2(aq) + Hg_2Cl_2(s) + 2Cl^-(aq) \quad EMF = 2.60\ V \quad (9)$$

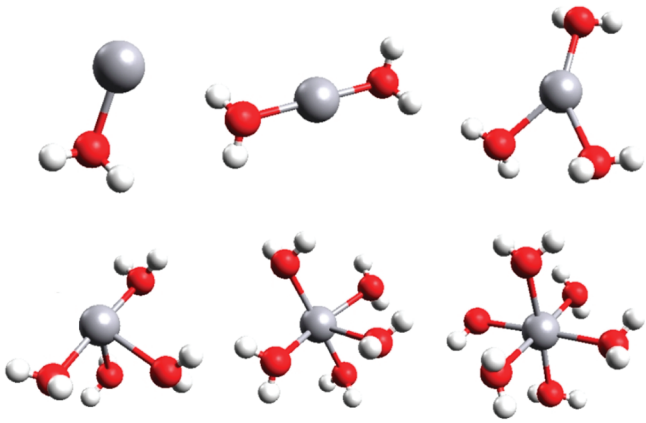

Figure 6. Optimized geometries of $Hg(H_2O)_m^{2+}$ ($m = 1-6$). Gray, red, and white spheres represent mercury, oxygen, and hydrogen, respectively.

TABLE 2: Selected Standard Gibbs Energies of Reaction, in Kilojoules per Mole, Involving Both Aqueous and Chlorinated Complexes of Mercury(II) and Mercury(I)

reaction	ΔG_r^0
$HgCl^+ + Cl^- \rightarrow HgCl_2$	−116
$HgCl_3^- \rightarrow HgCl_2 + Cl^-$	−21
$HgCl_4^{2-} \rightarrow HgCl_2 + 2Cl^-$	−41
$HgCl_5^{3-} \rightarrow HgCl_2 + 3Cl^-$	−128
$Hg(H_2O)^{2+} + H_2O \rightarrow Hg(H_2O)_2^{2+}$	−24
$Hg(H_2O)_3^{2+} \rightarrow Hg(H_2O)_2^{2+} + H_2O$	−41
$Hg(H_2O)_4^{2+} \rightarrow Hg(H_2O)_2^{2+} + 2H_2O$	−149
$Hg(H_2O)_5^{2+} \rightarrow Hg(H_2O)_2^{2+} + 3H_2O$	−169
$Hg(H_2O)_6^{2+} \rightarrow Hg(H_2O)_2^{2+} + 4H_2O$	−173
$Hg(H_2O)_2^{2+} + 2Cl^- \rightarrow HgCl_2 + 2H_2O$	−92
$Hg_2(H_2O)_2^{2+} + 2Cl^- \rightarrow Hg_2Cl_2 + 2H_2O$	−57
$Hg_2Cl_4^{2-} \rightarrow Hg_2Cl_2 + 2Cl^-$	−80
$2HgCl \rightarrow Hg_2Cl_2$	−168

$$2CO_2^{\bullet-}(aq) + 2HgCl_2(aq) \rightarrow 2CO_2(aq) + Hg_2Cl_2(s) + 2Cl^-(aq) \quad EMF = 2.66\ V \quad (10)$$

In the preceding processes, a reduction potential of −2 V was considered for $E(CO_2/CO_2^{\bullet-})$, according to ref 28. It should be also mentioned that the one-electron reaction

$$CO_2^{\bullet-}(aq) + HgCl_2(aq) \rightarrow CO_2(aq) + HgCl(aq) + Cl^-(aq) \quad (11)$$

is characterized in the present work by a standard Gibbs energy of −148.19 kJ mol^{-1} and an EMF of 1.54 V, in excellent agreement with the accepted value of 1.53 V, that can be deduced from reduction potentials given in refs 28 and 29.

To further validate the above results on standard Gibbs energies of reactions, standard Gibbs energies of formation of some selected species were also calculated. These are shown in Supporting Information Table S3.

Conclusion

The results depicted in Figure 4 show that the concentration of Hg(II) or total mercury can be drastically reduced upon irradiation with the laser ($\lambda^{exc} = 266$ nm) or with the mercury lamp.

If the method proposed in this paper is employed in the presence of chloride ions, even at low concentration as in the case of our experiments, $[Cl^-]_0 = 0.4$ mM for the experiments performed with deionized water and $HgCl_2$, and $[Cl^-]_0 = 2.8$ mM for the experiments performed with drinking water, the reduction of Hg(II) yields $Hg_2Cl_2(s)$, reaction 5. The low K_{sp} value for Hg_2Cl_2 allows the elimination of Hg(II) by centrifugation or decantation.

The reduction via $CO_2^{\bullet-}$could also be potentially applicable to other metal ions. For instance, the standard redox potentials $E^0(Pu^{5+}/Pu^{4+}) = 1.1$ V and $E^0(Pu^{4+}/Pu^{3+}) = 1.01$ V vs NHE tell us that the same procedure proposed here for Hg(II) could be employed to reduce Pu^{5+} to Pu^{3+}/ Pu^{4+}. The environmental advantage of reducing Pu^{5+} is based on the fact that Pu^{3+} and Pu^{4+} are more strongly sorbed on organic particles than Pu^{5+}.[38] Thus, reduction by $CO_2^{\bullet-}$ followed by treatment with organic particles could be used for eliminating Pu from waters.

Theoretical calculations show that both $HgCl_2$ and Hg_2Cl_2 should be involved in a two-electron reduction reaction with the carbon dioxide radical anion, a process that is characterized by an EMF = 2.41 V. This result agrees well with experimental findings concerning the observation of solid Hg_2Cl_2 upon irradiation of aqueous Hg(II) solutions in the presence of peroxodisulfate and formic acid. Moreover, calculations predict that the one-electron reduction of $HgCl_2$ to HgCl by the carbon dioxide radical anion should proceed with an EMF = 1.54 V.

Acknowledgment. This work was supported Grant PICT 2007 No. 00308 from Agencia Nacional de Promoción Científica y Tecnológica, (ANPCyT, Argentina), by the Italian Ministry of Foreign Affairs and the Università della Calabria. D.O.M. thanks the DAAD Alumni Program for an equipment grant. A.M.B. thanks CONICET (Argentina) for a graduate studentship. MCG and RPD are research members of CONICET, (Argentina). D.O.M. is a research member of Comisión de Investigaciones Científicas de la Provincia de Buenos Aires (CICPBA, Argentina).

Supporting Information Available: Tables showing physicochemical analysis of the drinking water employed in the experiments shown in the inset of Figure 4, geometrical parameters of some of the species studied in the present work and their comparison with data obtained from other sources, and standard Gibbs energies of formation for selected species studied in the present work and their comparison with experimental data. This material is available free of charge via the Internet at http://pubs.acs.org.

References and Notes

(1) Lin, C.-J.; Pehkonen, S. O. *Atmos. Environ.* **1999**, *33*, 2067–2079.
(2) Gårdfeldt, K.; Jonson, M. *J. Phys. Chem. A* **2003**, *107*, 4478–4482.
(3) House, D. A. *Chem. Rev.* **1962**, *62*, 185–203.
(4) Anipsitakis, G. P.; Dionysiou, D. D. *Environ. Sci. Technol.* **2003**, *37*, 4790–4797.
(5) Mora, V. C.; Rosso, J. A.; Le Roux, G. C.; Mártire, D. O.; Gonzalez, M. C. *Chemosphere* **2009**, *75*, 1405–1409.
(6) McElroy, W. J.; Waygood, S. J. *J. Chem. Soc., Faraday Trans.* **1990**, *86*, 2557–2564.
(7) Alegre, M. L.; Geronés, M.; Rosso, J. A.; Bertolotti, S. G.; Braun, A. M.; Mártire, D. O.; Gonzalez, M. C. *J. Phys. Chem. A* **2000**, *104*, 3117–3125.

(8) Neta, P.; Simic, M.; Hayon, E. *J. Phys. Chem.* **1969**, *73*, 4207–4213.
(9) Wine, P. H.; Tang, Y.; Thorn, R. P. *J. Geophys. Res., [Atmos.]* **1989**, *94* (D1), 1085–1094.
(10) Rosso, J. A.; Bertolotti, S. G.; Braun, A. M.; Mártire, D. O.; Gonzalez, M. C. *J. Phys. Org. Chem.* **2001**, *14*, 300–309.
(11) David Gara, P.; Bucharsky, E.; Wörner, M.; Braun, A. M.; Mártire, D. O.; Gonzalez, M. C. *Inorg. Chim. Acta* **2007**, *360*, 1209–1216.
(12) Wardman, P. *J. Phys. Chem. Ref. Data* **1989**, *18*, 1637–1755.
(13) Gårdfeldt, K.; Jonsson, M. *J. Phys. Chem. A* **2003**, *107*, 4478–4482.
(14) Caregnato, P.; David Gara, P. M.; Bosio, G. N.; Gonzalez, M. C.; Russo, N.; Michelini, M. C.; Mártire, D. O. *J. Phys. Chem. A* **2008**, *112*, 1188–1194.
(15) Ershov, B. G. *Russ. Chem. Rev.* **1997**, *66*, 93–105.
(16) Das, T. N.; Ghanty, T. K.; Pal, H. *J. Phys. Chem. A* **2003**, *107*, 5998–6006.
(17) Kuhn, H. J.; Braslavsky, S. E.; Schmidt, R. *Pure Appl. Chem.* **2004**, *76*, 2105–2146.
(18) Becke, A. D. *Phys. Rev. A* **1988**, *38*, 3098–3100.
(19) Lee, C.; Yang, W.; Parr, R. G. *Phys. Rev. B* **1988**, *37*, 785–789.
(20) Hohenberg, P.; Kohn, W. *Phys. Rev.* **1964**, *136*, B864–B871.
(21) Kohn, W.; Sham, L. J. *Phys. Rev.* **1965**, *140*, A1133–A1138.
(22) Parr, R. G.; Yang, W. *Density Functional Theory of Atoms and Molecules*: Oxford University Press: Oxford, U.K., 1989.
(23) Peterson, K. A.; Puzzarini, C. *Theor. Chem. Acc.* **2005**, *114*, 283–296.
(24) Figgen, D.; Rauhut, G. M.; Dolg, M.; Stoll, H. *Chem. Phys.* **2005**, *311*, 227–244.
(25) Dunning, T. H., Jr. *J. Chem. Phys.* **1989**, *90*, 1007–1023.
(26) Tomasi, J.; Mennucci, B.; Cammi, R. *Chem. Rev.* **2005**, *105*, 2999–3093.
(27) Frisch, M. J.; Trucks, G. W.; Schlegel, H. B.; Scuseria, G. E.; Robb, M. A.; Cheeseman, J. R.; Montgomery, Jr., J. A.; Vreven, T.; Kudin, K. N.; Burant, J. C.; Millam, J. M.; Iyengar, S. S.; Tomasi, J.; Barone, V.; Mennucci, B.; Cossi, M.; Scalmani, G.; Rega, N.; Petersson, G. A.; Nakatsuji, H.; Hada, M.; Ehara, M.; Toyota, K.; Fukuda, R.; Hasegawa, J.; Ishida, M.; Nakajima, T.; Honda, Y.; Kitao, O.; Nakai, H.; Klene, M.; Li, X.; Knox, J. E.; Hratchian, H. P.; Cross, J. B.; Bakken, V.; Adamo, C.; Jaramillo, J.; Gomperts, R.; Stratmann, R. E.; Yazyev, O.; Austin, A. J.; Cammi, R.; Pomelli, C.; Ochterski, J. W.; Ayala, P. Y.; Morokuma, K.; Voth, G. A.; Salvador, P.; Dannenberg, J. J.; Zakrzewski, V. G.; Dapprich, S.; Daniels, A. D.; Strain, M. C.; Farkas, O.; Malick, D. K.; Rabuck, A. D.; Raghavachari, K.; Foresman, J. B.; Ortiz, J. V.; Cui, Q.; Baboul, A. G.; Clifford, S.; Cioslowski, J.; Stefanov, B. B.; Liu, G.; Liashenko, A.; Piskorz, P.; Komaromi, I.; Martin, R. L.; Fox, D. J.; Keith, T.; Al-Laham, M. A.; Peng, C. Y.; Nanayakkara, A.; Challacombe, M.; Gill, P. M. W.; Johnson, B.; Chen, W.; Wong, M. W.; Gonzalez, C.; and Pople, J. A. *Gaussian 03*, Revision D.01; Gaussian: Wallingford, CT, 2004.
(28) Buxton, G. V.; Salmon, G. A.; Wood, N. D. In *Proceedings of the Fifth European Symposium on the Physico-chemical Behaviour of Atmospheric Pollutants*; Restelli, G., Angeletti, G., Eds.; Kluwer: Dordrecht, The Netherlands, 1990; p 245.
(29) Kozicki, M.; Filipczak, K.; Rosiak, J. *Radiat. Phys. Chem.* **2003**, *68*, 827–835.
(30) Tachikawa, T.; Tojo, S.; Fujitsuka, M.; Majima, T. *Langmuir* **2004**, *20*, 9441–9444.
(31) Das, T. N.; Ghanty, T. K.; Pal, H. *J. Phys. Chem. A* **2003**, *107*, 5998–6006.
(32) Powell, K. J.; Brown, P. L.; Byrne, R. H.; Gajda, T.; Hefter, G.; Sjöberg, S.; Wanner, H. *Pure Appl. Chem.* **2005**, *77*, 739–800.
(33) Si, L.; Ariya, P. A. *Environ. Sci. Technol.* **2008**, *42*, 5150–5155.
(34) Nazhat, N. B.; Asmus, K.-D. *J. Phys. Chem.* **1973**, *77*, 614–620.
(35) Pokrovskiy, O. S. *Geochem. Int.* **1996**, *33*, 83–97.
(36) Tam, K. Y.; Wang, R. L.; Lee, C. W.; Compton, R. G. *Electroanalysis* **1997**, *9*, 219–224.
(37) *CRC Handbook of Chemistry and Physics*, 72nd ed.; CRC Press: Boca Raton, FL, 1991−1992.
(38) Reilly, S. D.; Runde, W.; Neu, M. P. *Geochim. Cosmochim. Acta* **2007**, *71*, 2672–2679.

JP106035M